DINAME 2017 - Proceedings of the XVII International Symposium on Dynamic Problems of Mechanics
A. T. Fleury, D. A. Rade, P. R. G. Kurka (Editors), ABCM, São Sebastião, SP, Brazil, March 5-10, 2017

DINAME 2017 - Mechanical Synthesis and Analysis of a Four Bar Linkage

Eline Tiemi Shiino[1], **Leonardo Biagiotti Saint Martin**[2], **Katia Lucchesi Cavalca**[3]

[1, 2, 3] Laboratory of Rotating Machinery, Faculty of Mechanical Engineering, University of Campinas, 200 Mendeleyev Street, 13083-860, Campinas, São Paulo, Brazil

[1] elineshiino@gmail.com

[2] leonardo.saintmartin@gmail.com

[3] katia@fem.unicamp.br

Abstract: Planar mechanisms formed by four bars linked in a kinematic chain are the simplest and most versatile mechanisms, being generally found in several mechanical devices. Moreover, this type of mechanism has multiple exit movements, from a straight line to a circular shape, or a complex trajectory, allowing their use in the solution of various engineering's problems. As an example of application, four bar linkages are employed in the automotive suspension, arranged in parallel planes. In this paper, a computational algorithm in MATLAB was developed, utilizing classical methods of mechanical synthesis for four bar linkages, up to three precision points. This algorithm was subsequently utilized to the synthesis of a four bar linkage similar to an automotive suspension. A spring and a damper were positioned crosswise the mechanism. Lately, an analysis of the kinematics and kinetic of the suspension was accomplished. In the kinetic analysis, the mechanism was submitted to a force similarly to a car passing by an abrupt discontinuity on the road. Finally, the mechanical response of the system is analyzed and an optimization of the values of the stiffness of the spring and the damping factor of the shock absorber is carried on, seeking the minimization of the vibration effects.

Keywords: Mechanical synthesis, four bar linkages, kinematic and kinetic analysis, optimization.

INTRODUCTION

The synthesis of mechanisms investigates methods to design mechanisms according to specified kinematic and dynamic principles. These methods can be either graphical or analytical. The graphical methods provide the fastest and simplest techniques to determine the dimensions of a mechanism, usually working for up to three precision points. However, the analytical synthesis methods are algebraic, which make them suitable for implementation of algorithms in a computer. In this paper, the dimensional synthesis method employed was introduced by Freudenstein and Sandor (1959), being posteriorly developed by Erdman and Sandor (1997). Linear loop equations of the four bar mechanisms were written in their complex form, being then arranged in matrix form allowing the solution of a linear system, resulting in the mechanism's lengths of the bars.

Four bar mechanisms are formed by three motion links (two cranks connected by a coupler), and a fixed link, and can be designed to guide a wide variety of movements. Hrones and Nelson (1951) atlas of four bar coupler curves is a useful reference which can provide the designer with a starting point for further design and analysis. It contains about 7000 coupler curves and defines the linkage geometry for each of its Grashof crank-rocker linkages, emphasizing the variety of motions accomplished by this type of linkage, and so, the ample practical usages they may be applied to.

One example of application of the four bar mechanism is the automobile suspension. The motion of the car's wheels are controlled and guided by some combination of planar four bar linkages, arranged on duplicate to provide better overall control. The wheel is attached to the coupler of the linkage assembly, and its motion is along a set of coupler curves. The coupler curve of the wheel center is nearly a straight line over the smallest vertical displacement required. This is desirable as the idea is to keep the tire perpendicular to the ground for best traction. In this application, a non-Grashof linkage is acceptable, as full rotation of the wheel is not desired. A spring and a damper are placed crosswise the mechanism, to support the weight of the vehicle and provide a fifth, variable length "force link" which stabilizes the mechanism (Norton, 2010). Figure 1 illustrates this assembly, where the chassis of the car is the ground link, and the coupler is the link that carries the wheel.

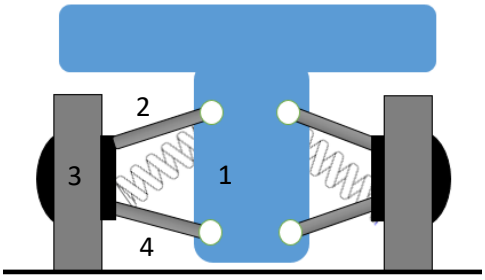

Figure 1 – Representation of the four bar linkage inspired in an automotive suspension.

In this paper, the center of mass of the coupler mechanism is the point of interest. An analysis of the kinematics and kinetic of this mechanism's point will be made, considering that the inertial system is positioned in the chassis, and the wheel is attached to the coupler's center of mass. Finally, an optimization is applied, aiming to determine the best damping factor of the shock absorber and stiffness of the spring. The objective is to minimize vibrations caused by the imperfections of the road. While the spring is responsible for the absorption of the impacts the wheels are subjected, the dampers control the spring motions, avoiding strong oscillations.

MATERIALS AND METHODS

Initially, the synthesis of the four bar linkage is made, as described by Norton (2010). The linkage is designed to pass a point of interest positioned on the coupler through three different points, defined by the position difference vectors $\boldsymbol{P}_{21}$, $\boldsymbol{P}_{31}$, with their respective directions δ_2, δ_3, and also rotate an angle α_2 between the first two precision points, and an angle α_3 between the first and the third precision points. Figure 2 illustrates a generic four bar linkage, in which $C_{1,1}$ refers to the first crank with angular position q in the first position, $C_{1,2}$ with rotation angle β_2 between the first and second positions and $C_{1,3}$ with rotation angle β_3 between the first and third positions. Similarly, $C_{3,1}$ is the second crank with angular position A_3 in the first position, $C_{3,2}$ with rotation angle γ_2 between the first and second positions and $C_{3,3}$ is the third position with rotation angle γ_3 between the first and third positions. The coupler is defined by vectors $\boldsymbol{Z}_1$ and $\boldsymbol{S}_1$, in the first position with angular position φ and ψ respectively, $\boldsymbol{Z}_2$ and $\boldsymbol{S}_2$, with an angular rotation of α_2 between the first and second positions, and $\boldsymbol{Z}_3$ and $\boldsymbol{S}_3$, in the third position with a rotation angle of α_3. $\boldsymbol{G}_1$ is the ground linkage, $\boldsymbol{P}_{21}$, δ_1, $\boldsymbol{P}_{31}$, δ_2 are translation and angular displacements of the point of interest in the second and third positions, respectively.

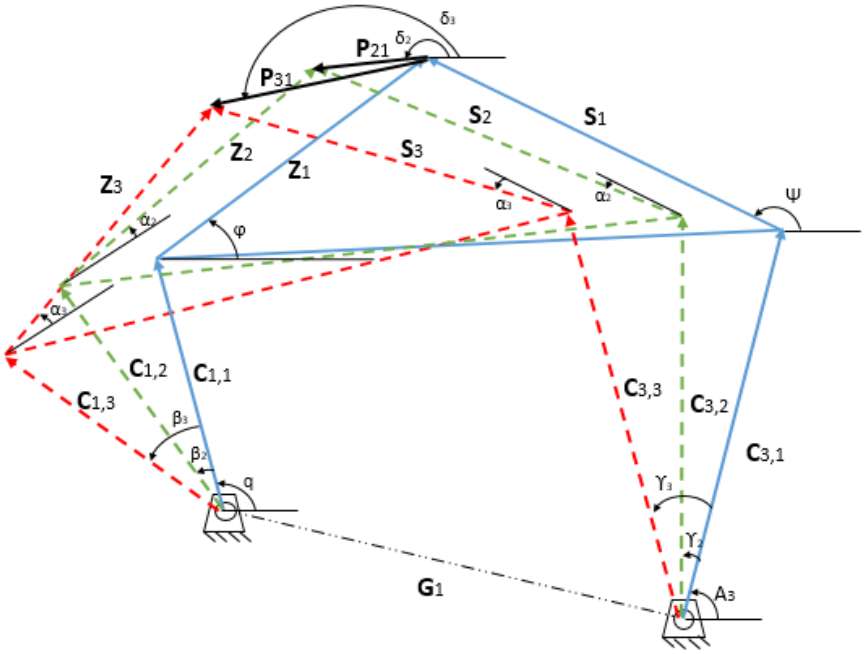

Figure 2 – Three position synthesis of a four bar linkage.

The loop equations on the left part of the mechanism, for the second and third positions, relatively to the initial position, are given by Eq. (1) and Eq. (2). The equations are initially given in vector form, and afterwards replaced by complex equivalents.

$$\boldsymbol{C}_{1,2} + \boldsymbol{Z}_2 - \boldsymbol{P}_{21} - \boldsymbol{Z}_1 - \boldsymbol{C}_{1,1} = 0 \rightarrow c_1 e^{j(q+\beta_2)} + z e^{j(\varphi+\alpha_2)} - p_{21} e^{j\delta_2} - z e^{j\varphi} - c_1 e^{jq} = 0 \quad (1)$$

$$\boldsymbol{C}_{1,3} + \boldsymbol{Z}_3 - \boldsymbol{P}_{31} - \boldsymbol{Z}_1 - \boldsymbol{C}_{1,1} = 0 \rightarrow c_1 e^{j(q+\beta_3)} + z e^{j(\varphi+\alpha_3)} - p_{31} e^{j\delta_3} - z e^{j\varphi} - c_1 e^{jq} = 0 \quad (2)$$

Separating the equations into real and imaginary parts results in four linear equations. Written in matrix form, the linear system to be solved is presented in Eq. (3).

$$\begin{bmatrix} (\cos\beta_2 - 1) & -\sin\beta_2 & (\cos\alpha_2 - 1) & -\sin\alpha_2 \\ (\cos\beta_3 - 1) & -\sin\beta_3 & (\cos\alpha_3 - 1) & -\sin\alpha_3 \\ \sin\beta_2 & (\cos\beta_2 - 1) & \sin\alpha_2 & (\cos\alpha_2 - 1) \\ \sin\beta_3 & (\cos\beta_3 - 1) & \sin\alpha_3 & (\cos\alpha_3 - 1) \end{bmatrix} \begin{pmatrix} c_1\cos q \\ c_1\sin q \\ z\cos\varphi \\ z\sin\varphi \end{pmatrix} = \begin{bmatrix} p_{21}\cos\delta_2 \\ p_{31}\cos\delta_3 \\ p_{21}\sin\delta_2 \\ p_{31}\sin\delta_3 \end{bmatrix} \tag{3}$$

Similarly, this procedure is accomplished in the right part of the mechanism, thus defining completely the dimensions of the four bar linkage, as well as its initial position. The next step is the kinematic analysis of the mechanism, as detailed by Doughty (1987). Figure 3 illustrates a generic four bar linkage.

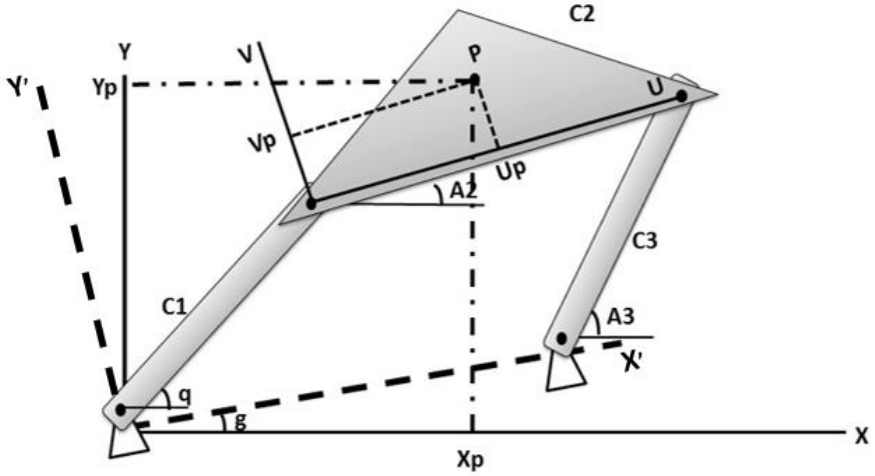

Figure 3 – Four bar linkage kinematic scheme and coordinate systems.

Loop equations of the linkage are required, given by Eq. (4) in x-axis and Eq. (5) in y-axis. C_1, C_2, C_3 and C_4 are the lengths of the four bars of the mechanism, and the respective angular positions are q, A_2, A_3 and g.

$$f_1(q, A_2, A_3) = C_1\cos(q) + C_2\cos(A_2) - C_3\cos(A_3) - C_4\cos(g) = 0 \tag{4}$$

$$f_2(q, A_2, A_3) = C_1\sin(q) + C_2\sin(A_2) - C_3\sin(A_3) - C_4\sin(g) = 0 \tag{5}$$

This system of equations is solved using the Newton-Raphson numerical method (Doughty, 1987), in order to determine the angular positions A_2 and A_3, for each given value of the angle q, the generalized coordinate of this mechanism. Partial differentiation of Eq. 4 and Eq. 5, with respect to the angles A_2 and A_3, gives the Jacobian of the system in Eq. 6.

$$\begin{bmatrix} \frac{\partial f_1}{\partial A_2} & \frac{\partial f_1}{\partial A_3} \\ \frac{\partial f_2}{\partial A_2} & \frac{\partial f_2}{\partial A_3} \end{bmatrix} = [J] = \begin{bmatrix} -C_2 sen(A_2) & C_3 sen(A_3) \\ C_2\cos(A_2) & -C_3\cos(A_3) \end{bmatrix} \tag{6}$$

Velocity kinematic coefficients K_2 and K_3 are presented in Eq. 7 (Doughty, 1987).

$$\begin{Bmatrix} K_2 \\ K_3 \end{Bmatrix} = \begin{Bmatrix} \dot{A}_2/\dot{q} \\ \dot{A}_3/\dot{q} \end{Bmatrix} = [J]^{-1} \begin{bmatrix} C_1 sin(q) \\ -C_1\cos(q) \end{bmatrix} \tag{7}$$

The acceleration kinematic coefficients L_2 and L_3 are calculated through differentiation of the velocity kinematic coefficients with respect to generalized coefficient q (Eq. (8)).

$$\begin{Bmatrix} L_2 \\ L_3 \end{Bmatrix} = [J]^{-1} \begin{Bmatrix} C_1.cos(q) + K_2^2.C_2.\cos(A_2) - K_3^2.C_3.\cos(A_3) \\ C_1.sin(q) + K_2^2.C_2.\sin(A_2) - K_3^2.C_3.\sin(A_3) \end{Bmatrix} \tag{8}$$

The displacement of the point of interest *P* situated in the coupler, as shown in Fig. 3, is described by Eq. (9) and Eq. (10).

$$X_p = C_1\,cos(q) + U_p\,cos(A_2) - V_p\,sen(A_2) \tag{9}$$

$$Y_p = C_1\,sen(q) + U_p\,sen(A_2) + V_p\,cos(A_2) \tag{10}$$

The kinetic analysis is the study of the forces that cause movement in the system. The four bar linkage is a mechanism with a single degree of freedom; therefore the Eksergian's equation of motion can be employed, as presented in Eq. (11). Solving this equation requires a numerical method, such as the Runge-Kutta fourth order method (Abramowitz and Stegun, 1964).

$$\mathcal{J}(q)\ddot{q} + \frac{1}{2}\frac{d\mathcal{J}(q)}{dq}\dot{q}^2 + \frac{dV(q)}{dq} = Q^{nc} \tag{11}$$

Where $\mathcal{J}(q)$ is the generalized inertia, q is the generalized coordinate, $V(q)$ is the potential energy due to the elastic force of the spring, and Q^{nc} is the non-conservative generalized force, which includes, in this paper, the dissipative force of the damper, and an external force applied to the coupler. Equation (12) presents the generalized inertia $\mathcal{J}(q)$, which is dependent of the masses of the bars (M_1, M_2, M_3) and their moments of inertia $(I_{1cm}, I_{2cm}, I_{3cm})$, and the kinematic coefficients K. There are two different kinematic coefficients on Eq. (12). K_2 and K_3 were defined by Eq. (7), K_{ix} and K_{iy} come from the derivation of the positions of the bars's center of mass, as defined in Eq. (13). Kinematic coefficients of the others bars are omitted here, but can be similarly defined. Equation (14) represents the centripetal coefficient, which is the derivative of the generalized inertia $\mathcal{J}(q)$ divided by 2; equation (15) brings the potential energy term and its derivative; Q^{nc} is the generalized non-conservative force, given by Eq. (16).

$$\mathcal{J} = \left((I_{1cm} + M_1(K_{1x}^2 + K_{1y}^2)) + \left(M_2\left(K_{2x}^2 + K_{2y}^2\right) + I_{2cm}K_2^2\right) + (I_{3cm} + M_3(K_{3x}^2 + K_{3y}^2))K_3^2\right) \tag{12}$$

$$K_{1x} = \frac{dX_{1cm}}{dq}, K_{1y} = \frac{dY_{1cm}}{dq} \tag{13}$$

$$\frac{1}{2}\frac{d\mathcal{J}(q)}{dq} = \left(M_2.\left(K_{2x}.L_{2x} + K_{2y}.L_{2y}\right) + I_{2cm}.K_2.L_2\right) + \left((I_{3cm} + M_3(K_{3x}^2 + K_{3y}^2).K_3.L_3\right) \tag{14}$$

$$V(q) = \frac{k.\Delta B^2}{2};\ \frac{dV(q)}{dq} = k(B - B_0)\left(\frac{dB}{dq}\right) = k.K_B.(B - B_0) \tag{15}$$

$$Q^{nc} = -c.K_D^2.\dot{q} + F_{ext} \tag{16}$$

The external force applied to the coupler is an impulsive force, which represents an impact, such as an abrupt discontinuity on the road. For an underdamped system, the response to an impulse applied to it is given by Eq. (17). In this expression $\hat{F}$ is the change in linear momentum at impact. Deriving this equation twice, the acceleration is obtained and given by Eq. (19). Therefore, the external force applied is the mass of the quarter car m multiplied by the acceleration $\ddot{x}(t)$ in Eq. (20).

$$x(t) = \frac{\hat{F}e^{-\zeta\omega_n t}}{m\omega_d}\ sin\omega_d t \tag{17}$$

$$\dot{x}(t) = \frac{dx}{dt} = \frac{\hat{F}e^{-\zeta\omega_n t}}{m\omega_d}[-\zeta\omega_n\, sin(\omega_d t) + \omega_d\, cos(\omega_d t)] \tag{18}$$

$$\ddot{x}(t) = \frac{d^2x}{dt^2} = \frac{\hat{F}e^{-\zeta\omega_n t}}{m\omega_d}[(\zeta^2\omega_n^2 - \omega_d^2)\, sin(\omega_d t) - 2\zeta\omega_n\omega_d\, cos(\omega_d t)] \tag{19}$$

$$F_{ext} = m.\ddot{x}(t) = \frac{\hat{F}e^{-\zeta\omega_n t}}{\omega_d}[(\zeta^2\omega_n^2 - \omega_d^2)\, sin(\omega_d t) - 2\zeta\omega_n\omega_d\, cos(\omega_d t)] \tag{20}$$

Revising the theory of vibration, to explain the variables presented in Eq. (20), the undamped natural frequency of a single-degree of freedom system is given by Eq. (21). Equation (22) represents the damped natural frequency, and Eq. (23) the damping ratio.

$$\omega_n = \sqrt{k/m} \tag{21}$$

$$\omega_d = \omega_n\sqrt{1 - \zeta^2} = \sqrt{(k/m)}.\sqrt{1 - \zeta^2} \tag{22}$$

$$\zeta = \frac{c}{2\sqrt{km}} \tag{23}$$

Isolating the terms of stiffness coefficient of the spring on Eq. (22), and the damping factor of the shock absorber on Eq. (23), we obtain Eq. (24) and Eq. (25).

$$k = \frac{\omega_d^2 m}{(1-\zeta^2)} \tag{24}$$

$$c = 2\zeta\sqrt{km} \tag{25}$$

An optimization based on interior point methods is applied to the problem, aiming the minimization of the vibrations on the coupler. The interior point methods are a class of algorithms that solves linear and nonlinear convex optimization problems, subject to equality and inequality constraints, as presented by Byrd *et al* (1999) and (2000). The objective function of the problem is the displacement curve's overshoot of the coupler, which is the maximum peak value of the response curve. The restrictions added are the settling time of the displacement curve of the coupler, a constant damped frequency and the range of the damping factor. The time settling is defined as the necessary time for the response curve of the system to reach and remain within the range of the final steady-state value (Ogata, 2010). In this paper, the settling time threshold defined was 2% of the response's peak value. The human body tolerance to vibration is inside the frequency range of 4 to 8 Hz. (Rao, 2008) Therefore, in this paper, the damped frequency is considered constant and equal to 4 Hz in the calculations. Furthermore, the range of the damping factor considered for the system is between 0,2 and 0,4, to provide good ride. (Gillespie, 1992). Considering these values, the range of the stiffness coefficient of the spring and the damping factor of the shock absorber are defined within Eq. (24) and Eq. (25).

RESULTS

Initially, the synthesis of the four bar linkage gave the dimensions of the four bar linkage, as well as the orientation of the bars. The design process required a mechanism able to control the paths of multiple points on the coupler, where the wheel was attached. The coupler curve should be nearly a straight line over the smallest vertical displacement required for this application, to guarantee tire contact patch. Figure 4 illustrates the synthetized mechanism, a parallel non-Grashof four bar linkage, and the representation of its usage as a suspension.

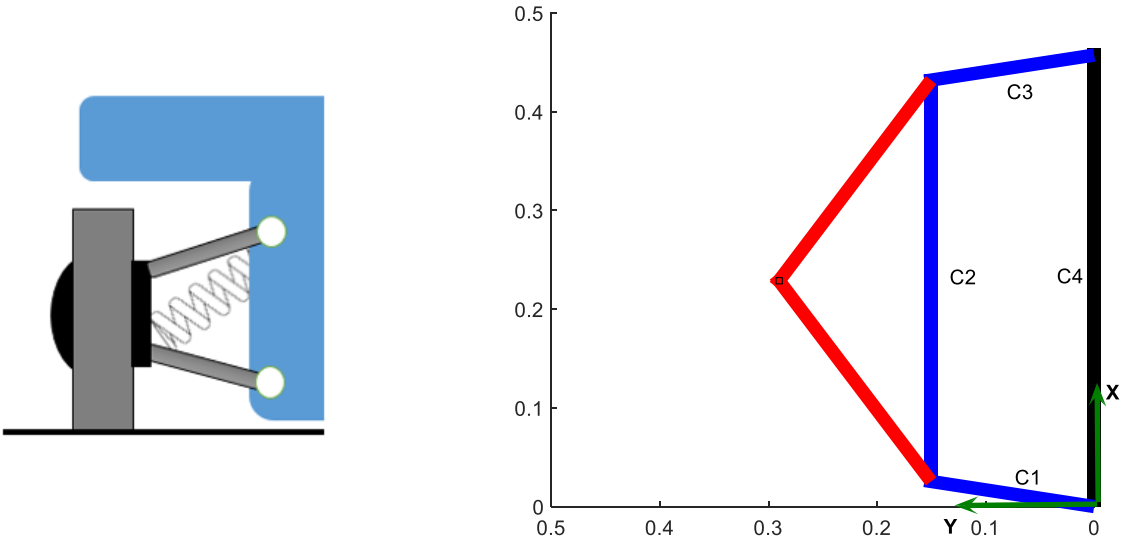

(a) **(b)**

Figure 4 – Four bar linkage
(a): Representation of the four bar linkage as an automotive suspension; (b): Synthetized mechanism

Table 1 presents the obtained lengths of the bars, their respective initial orientation, referenced in the X'Y' system in Fig. 3. The third column shows the angular variation of the C1 link (Δq) and C3 link (ΔA_3), as well as the inputs of angular velocity and acceleration of the C1 link. This information is used to obtain a kinematic analysis of the mechanism. The variation of these angles are illustrated in Fig. 5. It is important to notice that the variation of these angles are limited, as full rotation of the linkages is not desirable in this application.

Table 1 – Data input to the kinematic analysis of the mechanism.

Lengths of the bars	Orientation of the bars	Additional parameters
C1 = 152.4 mm	A1 = q = 80.40791°	$\Delta q = 40°$
C2 = 406.4 mm	A2 = 0°	$\Delta A_3 = 50°$
C3 = 152.4 mm	A3 = 99.5921°	$\dot{q} = 0.1\ rad/s$
C4 = 457.3 mm	A4 = 0°	$\ddot{q} = 0\ rad/s^2$

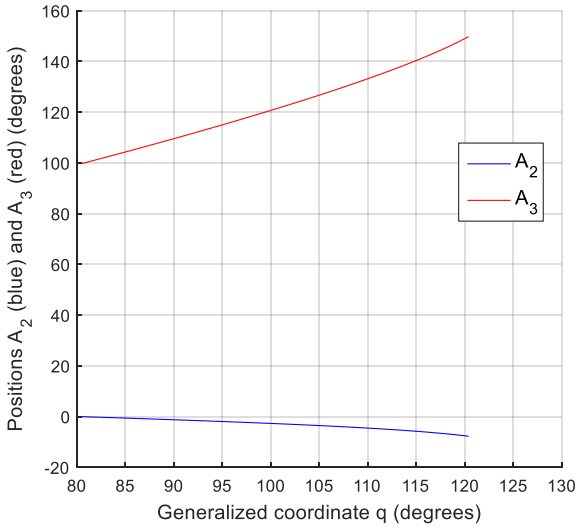

Figure 5 – Angular position of bars C_2 and C_3

The angular velocity and the acceleration can be obtained from velocity and acceleration coefficients (Equations (7) and (8)), being presented in Fig. 6.

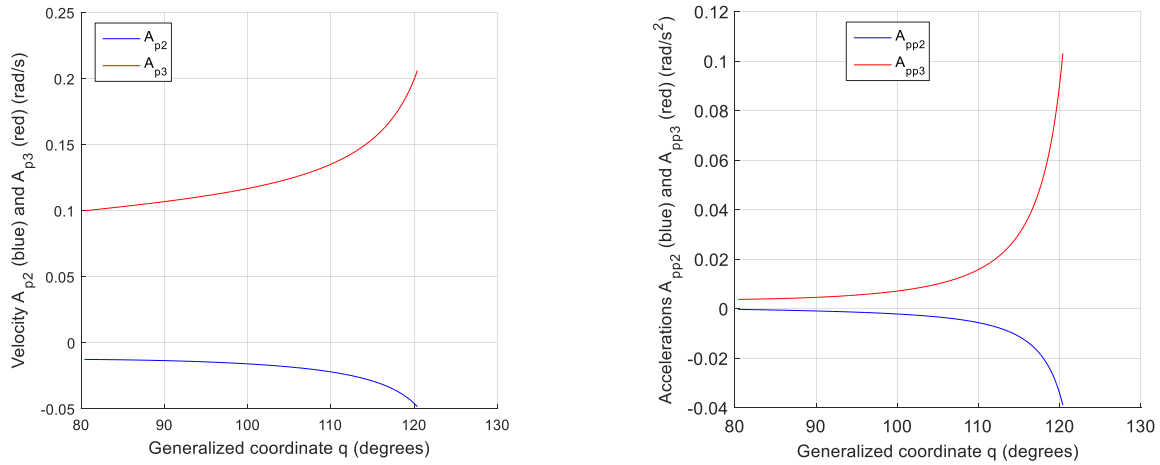

(a) (b)

Figure 6 – Angular position of the links
(a): Angular velocity of bars C_2 and C_3; (b): Angular accelerations of bars C_2 and C_3

The next step is the kinetic analysis of the mechanism, integrated to the whole system, and submitted to an external force on the coupler. For the kinetic analysis, further data of the mechanism is required, such as masses and inertia moments of the bars, and the Cartesian coordinates of the mass centers, relatively to the XY reference system. The mass of the car was assumed 1000 kg, dividing this value by four, considering a simplified quarter model car. These values are presented in table 2, and were provided by Peres (2012).

Table 2 – Cartesian coordinates of the centers of mass of the bars, and their physical properties.

X	Y	Masses	Inertia moments
X_{cm1} = 25 mm	Y_{cm1} = 81.6 mm	M_1 = 0.525 kg	Icm_1 = 0.057 kg.m^2
X_{cm2} = 249.9 mm	Y_{cm2} = 212.5 mm	M_2 = 1.05 kg	Icm_2 = 0.011 kg.m^2
X_{cm3} = 482.3 mm	Y_{cm3} = 81.6 mm	M_3 = 0.525 kg	Icm_3 = 0.057 kg.m^2

Figure 7 illustrates the acceleration of the coupler bar, as given by Eq. (19). The external force applied to the system is obtained multiplying this acceleration by the mass of the quarter model car. This external force, applied in the X direction, aims to simulate the passage of the vehicle through an abrupt discontinuity in the road.

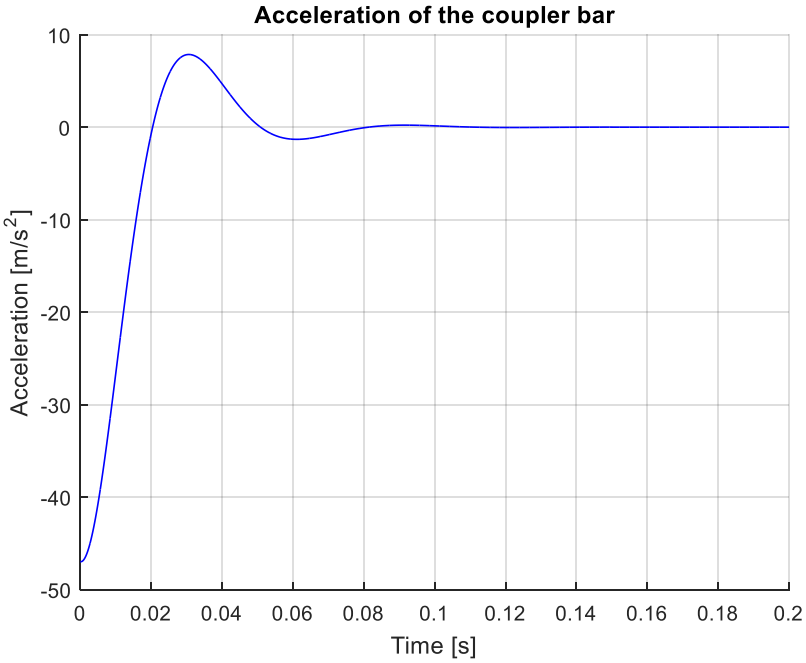

Figure 7 – External force applied to the coupler of the linkage.

The response of the system to this applied force is given by solving Eksergian's equation of motion presented in Eq. (11). The numerical solution employed to this problem was the fourth-order Runge-Kutta method, implemented in MATLAB by Saint Martin (2014), and developed by Abramowitz and Stegun (1964). The displacement curve of the center of mass of the coupler, as a response to the applied force is illustrated in Fig. 8. The center of mass of the coupler was chosen as the point of interest because it is assumed that the wheel is attached to the mechanism at this point. Furthermore, the force is considered to be applied to the system at this location. It is noticeable that the horizontal component is almost null when compared to the vertical component of the displacement. Nonetheless, the minimization of the vibrations of the coupler will be applied to its resultant displacement.

Figure 8 (a) illustrates the response of the system assembled with a spring with stiffness coefficient of k = 90000 N/m and shock absorber with a damping factor of c = 750 N.s/m. These values were provided by Peres (2012). However, for these values, the damping ratio was 0,0791, outside the desired range for a good ride. Moreover, the damped natural frequency obtained was about 3 Hz. Figure 8 (b) illustrates the response curve for *k* and *c* optimized values within the ranges defined of damping ratio (in this case, 0,3523) and damped natural frequency of 4 Hz.

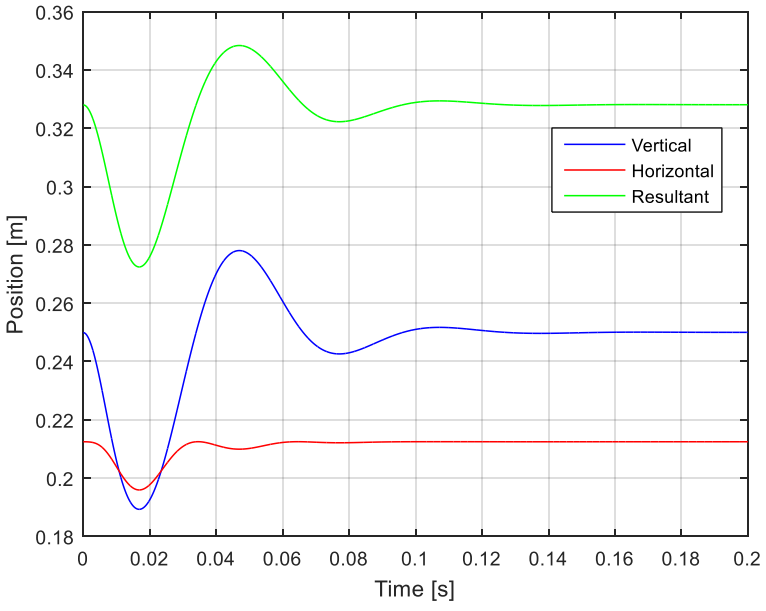

(a)

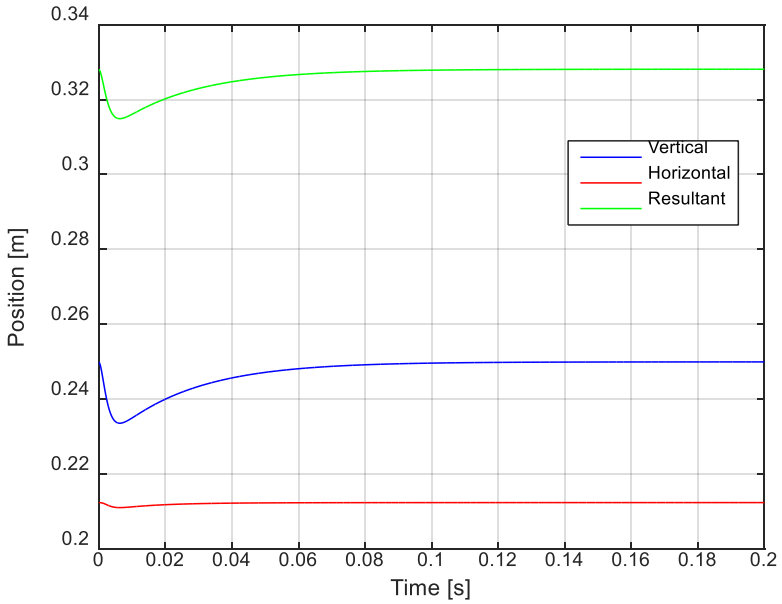

(b)

Figure 8 – Position of the center of mass of the coupler.
(a): Original suspension response; (b): Optimized response.

The variables to be optimized are the stiffness of the spring and the damping factor of the shock absorber. Figure 9 illustrates the variation of the maximum relative resultant displacement peaks within a range of different combinations of stiffness and damping. It is possible to notice that the maximum value of the overshoot decreases with the rise of the stiffness coefficient and the damping factor. Therefore, it is necessary to introduce further restrictions to the optimization problem; otherwise, the optimum values to the minimization of the displacement of the curve would always be the maximum values of stiffness and damping defined in the problem.

The restrictions added are the time settling of the system, the constant damped frequency and the range of the damping ratio. For higher frequencies, the stiffness coefficient of the spring increases, as well as the damping factor of the absorber, and consequently, the overshoot reduces. However, the human tolerance for vibrations is within the range of 4 to 8 Hz. The ideal comfort frequency for the passenger is the lowest possible within the acceptable range. Accordingly, resorting Eq. (24) and Eq. (25), considering the damped frequency to be constant and equal to 4 Hz, and the range of the damping factor between 0,2 and 0,4, the range of the variables to be optimized is defined as presented in table 3.

Table 3 – Optimization inputs and results

	Interval of optimization		ω_d[Hz]
	Lower Bound	**Upper Bound**	
Ksi	**0,2**	**0,4**	
K [N/m]	164493	187992	**4**
C [N.s/m]	2565	5484	**4**

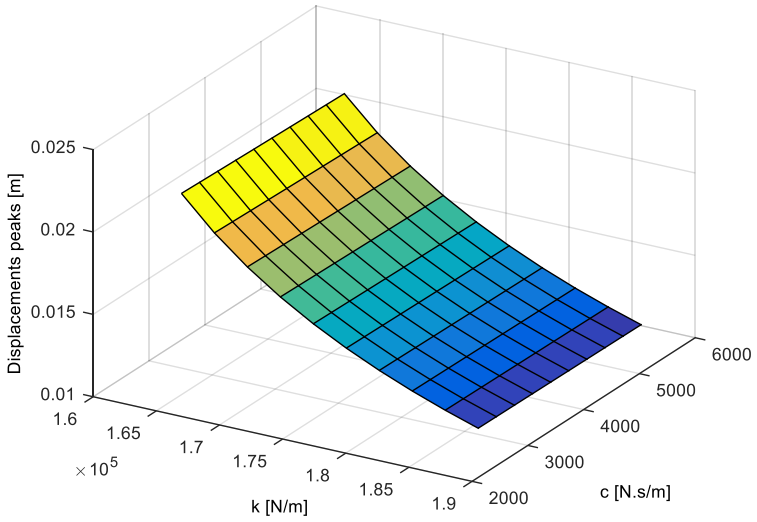

Figure 9 – Variation of the maximum peak of the response curve (resultant displacement of the center of mass of the coupler) with respect to the damping factor and the stiffness of the spring.

The optimization presented in this paper considered the minimization of the maximum amplitude of the point of interest position. For different values of settling time, and the same start point for the optimization, as well as the values for the lower and upper bounds for stiffness and damping coefficients (as presented in table 3), and a constant damped frequency of 4 Hz. The start point chosen is close to the lower bound defined. Due to the other restrictions added to the problem, such as the settling time, the damping factor range and the constant damping frequency, these values did not reach the highest values possible. Table 4 presents the starting points, as well as the optimum coefficients returned from the optimization process.

Table 4 – Optimization inputs and results

Tss [s]	Start Point [k0; c0] [N/m; N.s/m]	Optimum Point [k; c] [N/m; N.s/m]	Overshoot [m]	ζ	ω_d [Hz]
0,05	[164500, 2566]	[164500,8405; 2566,5483]	0,02182	0,2001	4
0,075	[164500, 2566]	[170347,9914; 3526,2333]	0,0169	0,2702	4
0,1	[164500, 2566]	[180283,9833; 4729,7261]	0,01319	0,3523	4
0,125	[164500, 2566]	[187992,2303; 5484,3924]	0,01153	0,4000	4

Figure 10 illustrates the displacement of the mass center of the coupler, for different optimum values, as well as the original displacement curve for the values provided by Peres (2012). The resultant displacement curve is referenced at the equilibrium position of the system to use the function *findpeaks* from MATLAB, it only considers positive peaks values. It is noticeable that the higher the settling time, the smaller the maximum peak of displacement. Furthermore, the damping ratio remains between the range given initially for the problem, and it is directly proportional to the time settling. Because of the damping ratio range, higher values of settling time were not possible, as the optimum coefficients obtained reached the upper bound defined.

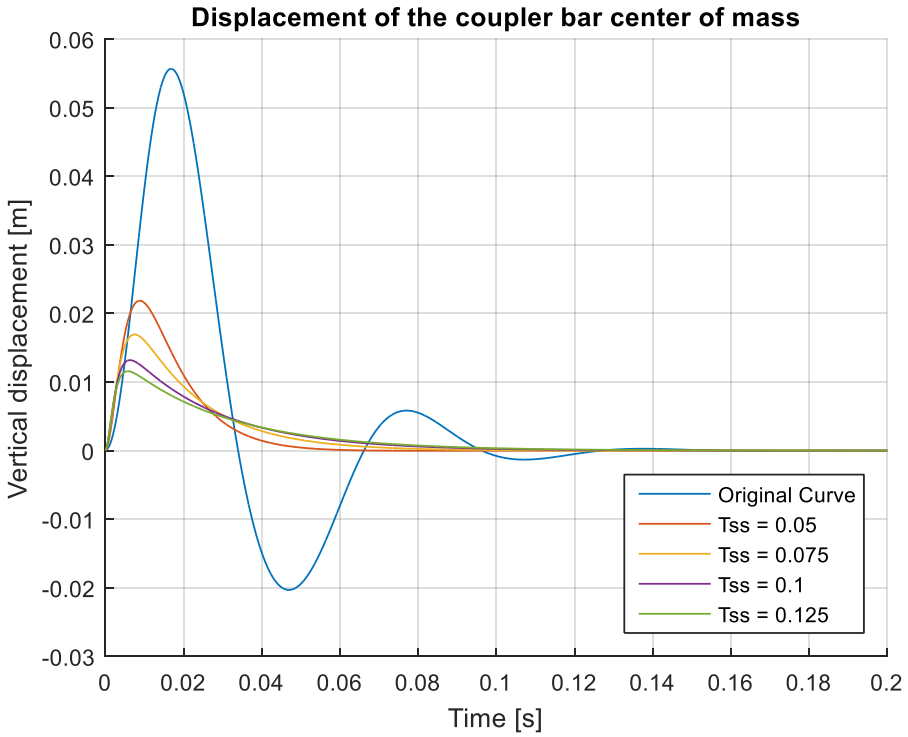

Figure 10 – Displacement of the coupler's center of mass

CONCLUSION

In this paper, a four bar mechanism was synthetized utilizing an analytical three precision point method developed by Erdman and Sandor (1997), thus calculating the lengths of the bars. Then, an analysis of the kinematics and kinetic of the mechanism point of interest in the coupler, in which it is considered that the wheel is attached, was made.

Positioning a damper and a spring crosswise the mechanism, and applying a force to the system, an optimization was realized, to determine the best damping factor of the shock absorber and stiffness of the spring. The objective function to the optimization was the minimization of the displacement curve of the interest point in the coupler, subject to a constant damped frequency of 4 Hz and a range of the damping factor between 0,2 and 0,4. These values were defined to provide a good comfort ride to the passenger, as found in literature. Another restriction to the problem was the time settling of the system, to guarantee its response would reach and remain within a pre-defined range around the final steady-state value.

The maximum overshoot and the settling time conflict with each other, meaning that they cannot be made smaller simultaneously. On the other hand, the damping factor is directly related to the settling time of the system. For smaller values of the settling time, the overshoot increased. Comparing the optimized curves to the original system, the overshoot

suffered a reduction of 60% to 76%, depending on the settling time chosen. For the settling time values, these did not vary much from the original system, which was of 0,1126s. Therefore, the best combination of the optimized coefficients was obtained with the settling time of 0,1s, which was close to the initial system, however with a reduction of 76,3% of the overshoot, and a damped natural frequency and damping ratio within the range stipulated. The optimum values of stiffness coefficient and damping factor depends on the project necessity, such as the type of car being designed, budget availability, the kind of effort the car is going to be submitted to, the transmissibility of vibrations to the passenger. The optimization process presented in this paper and its responses are a preliminary result of a work in progress, and it is still being refined.

ACKNOWLEDGMENTS

The authors would like to thank MSc. Thales Freitas Peixoto for his contribution to this work. Also, the authors thank the National Counsel of Technological and Scientific Development (CNPq) and CAPES for the financial support of this project.

REFERENCES

Abramowitz, M., and Stegun, L. A., 1964, Handbook of Mathematical Functions, Washington, D. C.: National Bureau of Standards, Applied Mathematics Series 55, US Government Printing Office.

Byrd, R. H., Gilbert, J. C., and Nocedal J., 2000, A Trust Region Method Based on Interior Point Techniques for Nonlinear Programming. Mathematical Programming, Vol 89, No. 1, pp. 149–185.

Byrd, R. H., Hribar, M. E. and Nocedal, J., 1999, An Interior Point Algorithm for Large-Scale Nonlinear Programming. SIAM Journal on Optimization, Vol 9, No. 4, pp. 877–900.

Doughty, S., 1987, Mechanics Of Machines, John Wiley & Sons.

Erdman, A. G., and Sandor, G. N., 1997, Mechanism Design: Analysis and Synthesis, Vol. 1, Prentice Hall: Upper Saddle River, NJ.

Freudenstein, F., and Sandor, G. N., 1959, Synthesis of Path Generating Mechanisms by Means of a Programmed Digital Computer, ASME Journal for Engineering in Industry, 81, p. 2.

Gillespie, T. D., 1992, Fundamentals of Vehicle Dynamics, Society of Automotive Engineers Inc.

Hrones, J. A., and Nelson, G. L., 1951, Analysis of the Four Bar Linkage, MIT Technology Press: Cambridge, MA.

Inman, D. J., 2007, Engineering Vibration, 3rd edition, Prentice Hall, Upper Saddle River, New Jersey, United States of America.

Norton, R. L., 2010, Design of Machinery, An Introduction to the synthesis and Analysis of Mechanisms and Machines, 4th edition, McGraw Hill Education.

Ogata, K., 2010, Modern Control Engineering, 5th edition, Prentice Hall, Upper Saddle River, New Jersey, United States of America, 905 p.

Peres, L. H. Y., 2012, Application Study of a Symmetrical Coupler in a Four Bar Mechanism, University of Campinas, Faculty of Mechanical Engineering.

Rao, S. S., 2008, Mechanical Vibrations, 4th edition, Pearson Prentice Hall.

Saint Martin, L. B., 2014, Kinematic and Kinetic Analysis of Generic Four Bar Mechanisms, University of Campinas, Faculty of Mechanical Engineering.

RESPONSIBILITY NOTICE

The authors are the only responsible for the material included in this paper.